Mechanical Behaviour of Macroscopic Interfaces for 3D Printed Multi-material Samples

Vasile Ermolai[1*,2][0000-0001-5967-5748], Alexandru Sover[2][0000-0003-3408-898X], Marius Andrei Boca[1,2][0000-0001-8560-1355], Adelina Hrițuc[1][0000-0003-3871-7800], Laurențiu Slătineanu[1][0000-0002-5976-9813], Gheorghe Nagîț[1][0000-0001-9649-8525] and Răzvan Cosmin Stavarache[1][0000-0001-6341-8277]

[1] "Gheorghe Asachi" Technical University of Iasi, Department of Machine Manufacturing Technology, Blvd. Dimitrie Mangeron 59A, Iasi, 700050, Romania
[2] Ansbach University of Applied Science, Faculty of Technology, Residenzstraße 8, Ansbach, 91522, Germany
*vasile.ermolai@hs-ansbach.de

Abstract. The development of 3D Printing technologies introduced new possibilities regarding multi-material part production. Fused Filament Fabrication (FFF) is one of those technologies suitable for multi-material 3D printing. Usually, multi-material parts are manufactured from different blends of the same material, also known as multi-colour 3D printing, or from materials with good chemical compatibility. Conventionally, a simple face-to-face bond interface between parts' bodies and a chemical bond between thermoplastics define the mechanical performance of multi-material components. In this regard, the paper aimed to investigate the strength of the contact interface of multi-material specimens using a geometrical approach. Therefore, multiple interlocking interfaces were investigated, such as omega shape, T-shape, dovetail, and others for samples made of low-compatibility thermoplastic materials, acrylic styrene-acrylonitrile (ASA), thermoplastic polyurethane (TPU). The results showed that macroscopic interlocking interfaces are significantly increasing the mechanical properties.

Keywords: Fused Filament Fabrication, Multi-material, Interlocking Mechanism, Contact Interface, Contact geometry.

1 Introduction

Fused Filament Fabrication (FFF) is a 3D printing technology that uses molten thermoplastic forced through a nozzle to build parts additively. First, a three-dimensional mesh is needed, processed in the machine's software (also known as the slicing tool), and then sliced in layers with a defined height. Multiple parameters must be adjusted based on the part's requirements (e.g., material, use), such as layer height, wall thickness, infill pattern and degree, deposition speed, and extrusion temperature [1].

Due to the good dimensional accuracy and material sourcing, FFF has become one of the most used 3D printing technologies. FFF can use standard materials, engineering-grade (e.g., acrylic styrene acrylonitrile-ASA), and high-performance polymers [2].

Multi-extrusion 3D printers allowed for more freedom in designing complex models and build orientation during printing by using soluble or low-compatibility materials for support structures and offered new opportunities to manufacture multi-colour and multi-material components. A multi-material part requires a distinct mesh for each material and is necessary to use chemically compatible materials (e.g., ABS-ASA) with similar melting ranges. Depending on the part's design, the materials can be deposited side by side, layered, or both [3].

Ermolai et al. studied the influence of contact interface geometry on the mechanical properties of multi-material samples made of two PLA blends [4]. The results show that the contact interface influences the tensile properties together with an overlap degree between the mating bodies.

Ribeiro et al. evaluated the performance of contact interfaces for multi-material of high-compatibility materials, PLA-PLA, and low-compatibility materials, PLA-TPU, for tensile strength [5]. They concluded that macroscopic geometry is necessary to achieve good mechanical properties.

Experimental research on the joint quality between additively manufactured samples made of two materials was performed by Kluczyński et al. [6]. Experimental results revealed that test samples with an overlapping joint have higher strength than joints with smooth surfaces.

This paper aims to study the mechanical performance of dissimilar-material samples from the geometrical perspective. Therefore, the study consists of six macroscopic contact interfaces and three interlocking degrees. The resulting geometries were systematised using the Taguchi method.

2 Methods

Multi-material components result from merging two or more bodies of the same part. Conventionally, the mating surfaces have a simple planar or circular profile. When simulating the printing process, based on the slicing tool preview, the mating bodies have only regions of vertical bond (see Fig. 1a). However, the resulting parts also present zones of horizontal bond, and an overlap between the part's bodies positively influences bond formation [4]. As a benchmark for the experimental plan's samples, a group of specimens was printed with a 0.4 mm overlap between the bodies (see Fig. 1b).

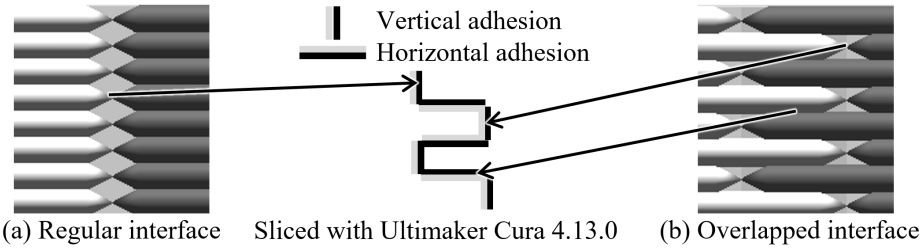

Fig. 1. Multi-material bond preview: a) Regular interface vs (b) 0.4 mm Overlapped interface.

For this study, two materials were considered, a natural colour TPU (i.e., Innovatefil TPU Hardness + from SmartMaterials3D) and a black colour ASA (i.e., ApolloX from FormFutura). Except for the printing temperature and the materials' cooling degree, all printing parameters were constant (see Table 1).

Table 1. Constant and variable parameters of the multi-material specimens.

Constant parameters				Variable parameters						
Layer thickness (mm)	0.2	Infill pattern	Grid	Level	I	II	III	IV	V	IV
Line width (mm)	0.4	Infill density	40	Contact geometry (CG)	OA	DT	DTA	TS	TSA	AS
Wall line count (no.)	4	Printing speed (mm/s)	35	Interlocking side (IS)	*Fyz*	*Pyz*	*Pyz & Pxz*			
Top/Bottom layers (no.)	5	Retraction distance (mm)	7	Overlap (Ovp.)	0.0	0.1	0.2			
Printing temp. (°C)	245/ *225*	Retraction speed (mm/s)	35	Abbreviations:			Dovetail adapted			- **DTA**;
Bed temp. (°C)	90	Fan speed (%)	1/*20*				T shape			- **TS**;
				Omega adapted	- **OA**;		T shape adapted			- **TSA**;
				Dovetail	- **DT**;		Arrow shape			- **AS**.

**Italic font for TPU Hardness+ material settings.*

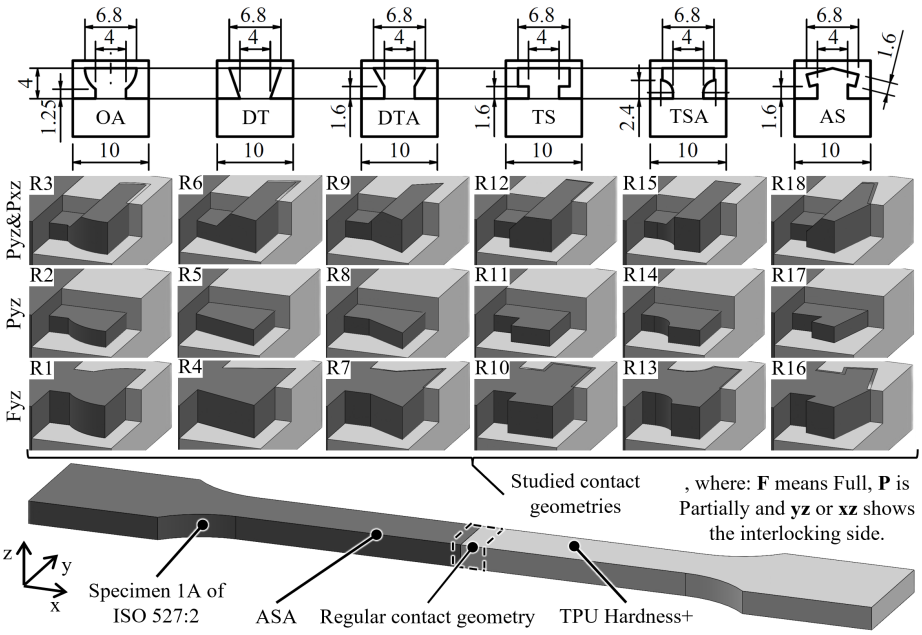

Fig. 2. Regular mating interface for head-to-head contact of multi-material samples vs macroscopic contact interfaces used in the experimental plan with their geometrical description and partial breakout of the studied contact interfaces.

A mixed Taguchi L18 matrix was for the experimental plan, with one factor at six-level and two factors at three levels. The considered variables are *Contact geometry*, *Interlocking side*, and *overlap* between mating regions (see Table 1).

The first variable describes the shape of the interlocking designs. These are *Omega adapted-OA*, *Dovetail-DT*, *Dovetail-adapted-DTA*, *T-shape-TS*, *T-shape-adapted-TSA*, and *Arrow shape-AS*.

The second parameter controls the interlocking side of each design, referred to printer's coordinate system. This way, *Fxy* provides contact on the entire sample's thickness, and *Pyz* ensures the contact only in the sample's core (i.e., 2 of 4 mm) with the mating body acting as an envelope. The last level, *Pyz*&Pxz, gives an additional interlocking region in the *xz* plane (e.g., R1 to R3 configurations from Fig. 2).

The third factor adjusts the overlap between the mating bodies. The overlap degree should positively influence the mechanical properties of the resulting samples.

Based on the experimental matrix, 18 macroscopic interlocking designs have resulted and numbered from R1 to R18 (see Fig. 2). The geometries were designed for sample 1A of ISO 257:2 for the tensile test, respectively specimen 1 of ISO 179:1 for the impact test. The interfaces have a 4 mm base and height for the male body and a 1.6 mm sidewall thickness (i.e., four extrusion lines) for the female body.

The rest of the dimensions were constrained to have a minimum 1.6 mm wall thickness. The resulting geometries are presented in Fig. 2.

Tensile tests were performed using an Instron 4411 uniaxial testing machine with a load capacity of 5kN. The impact strength was determined using a Zwick 5102.21 Charpy test machine using a 2J pendulum. All samples were manufactured using an Ultimaker 3 printer in a closed environment after reaching 40°C. Four replicates were printed for each run covered in the experimental plan for the tensile test and ten samples for the impact test. The average tensile and impact strength test results were analysed using the Minitab 21.1 statistical tool.

3 Results and discussion

The results include studying the specimens' tensile and impact strength with their response discussion, referable to the benchmark set of samples. The considered factors' influence was analysed using graphical representation and variance of the responses of the mechanical tests.

Regarding the tensile test results, all specimens presented a similar failure mode in each group (e.g., *OA*, *DT*). Furthermore, breaking behaviour was also comparable between interlocking interface sides. Samples with *Fyz* geometry failed in the TPU material side and broke in the upper side of the contact interface in the thinnest section of the female body. In the R13 group, samples did not detach entirely and were held together by *TS* interlocking geometry (see Fig. 3). For specimens partially interlocked in the *yz* plane (i.e., *Pyz*), the breaking regions appeared in the ASA material side or inside the TPU body (e.g., R8 trials). As for the configurations with *Pyz&Pxz* interlocking sides, specimens broke at the bottom (e.g., R3, R6, setups) or at the top region of the

contact geometries (e.g., R12 group). Examples of the failure mode of the contact interfaces and stress-strain curves are presented in Fig. 3.

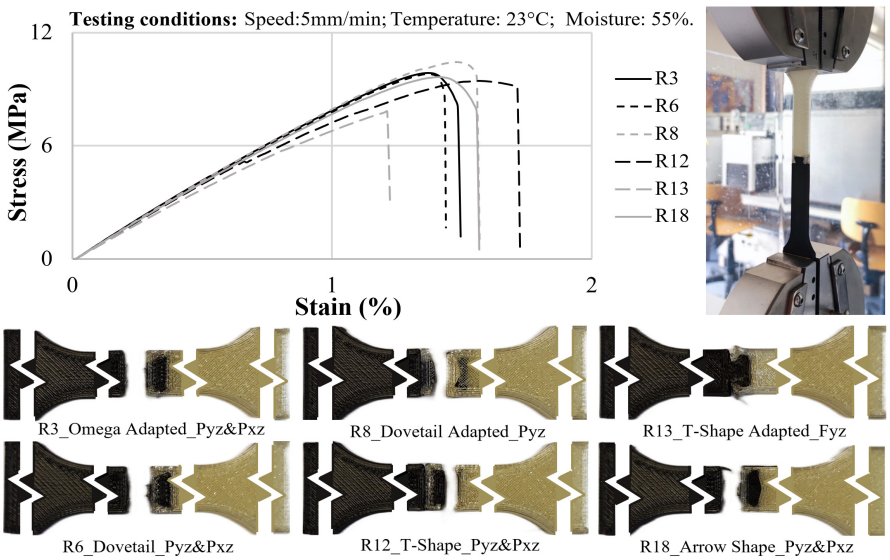

Fig. 3. Stress-strain curves of R3, R6, R8, R12, R14, and R18, and their failure mode.

All samples were tested for flatwise orientation for the Charpy test and showed similar failure modes for each group of specimens. *Fyz* interlocking side broke samples at the top of the contact geometry on the TPU material side. As for the other interlocking sides, samples failed at the bottom side of the male body, at the thinnest section of the ASA body. The TSA group registered the highest impact strength, followed by the AS group. The samples with Fyz interlocking side showed the highest energy absorption capacities, for which the interface bottom of the ASA body had the thickest cross-sections (see Fig. 4).

After the mechanical tests, the raw data was used to determine the average stress and strain at peak impact strength for each group of specimens, including the benchmark samples. The average results were analysed graphically using clustered column charts (see Fig 4). The results are relevant, presenting minor standard deviations. Overall, stress averages display a standard deviation in the range (0.11, 1.08 MPa) and the strain whiting the interval (0.03, 0.34 %). As for the impact strength, the standard deviation is in the (0.08, 0.89 kJ/mm^2) range.

All six macroscopic interlocking geometries registered an increase in load capacity and maximum yield in tensile strength. As presented in Fig. 4, the weakest of the considered designs was the arrow shape with *Fyz* and *Pyz* interlocking sides. The average results show a slight variation between the studied shapes and the interlocking sides for the rest of the specimens. Overall, the best results were obtained for the R8 configuration with DTA profile, Pyz interlocking, and 0.2 mm overlap between mating bodies for the tensile strength. As for the yield, the *TSA* interface with *Pyz&Pxz* interlocking

showed the best results. According to the main effects plots (see Fig. 5), the optimum stress-strain ratio can be achieved using a TS interface with a *Pyz&Pxz* interlocking and 0.1 mm overlap between the sample's bodies.

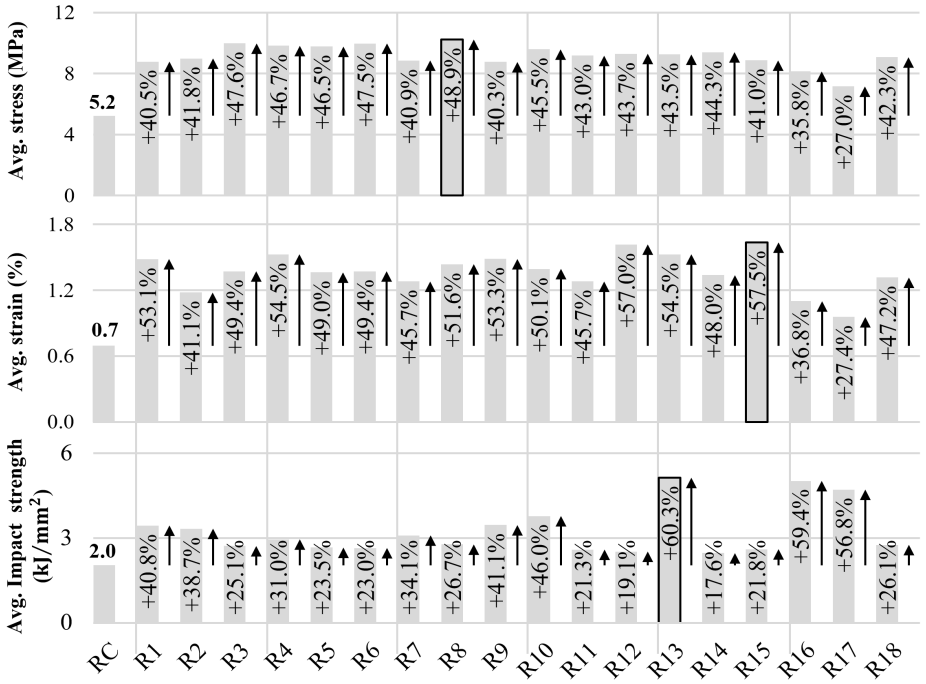

Fig. 4. Average tensile stress and strain at peak and impact strength of the experimental runs referred to the regular contact interface specimens with 0.4 mm overlap.

All considered contact geometries showed increased energy absorption capacity regarding the impact strength, referable to the benchmark. Except for the *DTA* group, the *Pyz&Pxz* interlocking side showed the highest impact strength, and the rest of the studied contact interfaces obtained the best result for the *Fyz* interlocking side. A possible reason for these results is the larger cross-section area of the interlocking material in the sample's male body. Analysing the main effects diagrams (see Fig. 5) results that the highest energy absorption is achieved by *AS* contact interface followed by *TSA* with *Fyz* interlocking and with an insignificant influence of the overlap factor.

Firstly, the influence of the considered factors and first-level interactions was analysed using a graphical representation of the main effects and the Pareto charts of the standardised effects (see Fig. 5). Further, the factors' significance was appreciated based on F-Values and P-Values resulting from the analysis of the variance of the average mechanical properties (see Table 2). Except for *Ovp*CG*, other interactions were ignored due to low significance. The responses analysis helped identify the interlocking geometry's most significant variables for the mechanical properties. The analysis was performed with a risk factor α of 0.05 for all responses (see Fig. 5).

Table 2. F-Value and P-Value for main factors and significant interactions based on the analysed responses for the ASA-TPU specimens.

Response	Avg. stress		Avg. strain		Avg. Impact strength	
Factor	F-Value	P-Value	F-Value	P-Value	F-Value	P-Value
Ovp	7.59	0.051	1.63	0.270	0.01	0.916
CG	2.87	0.172	5.40	0.064	1.06	0.491
IS	1.50	0.326	11.61	0.022	3.13	0.152
Ovp*CG	0.95	0.533	2.73	0.176	0.54	0.743

As shown in Table 2 and Fig. 5, the significance of main factors and interactions differs depending on the analysed responses. The most important factor for average strain is the overlap between mating bodies, followed by the interlocking side and the interaction between the first two. The most significant factors for the strain and impact strength are the interlocking side, followed by the contact geometry, the *Ovp*CG* interaction and the overlap. Overall, the contact geometry and the interlocking side have the most significant influence on the mechanical properties of the ASA-TPU samples.

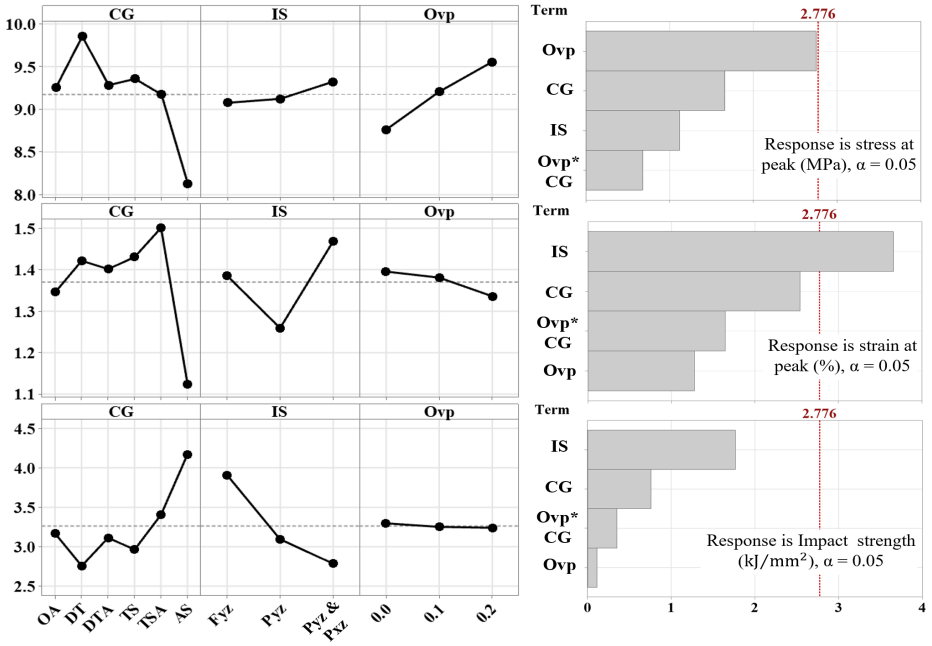

Fig. 5. Main effects plots of tensile stress, strain and impact strength, and Pareto chart of the standardised effects for the ABS-TPU samples.

The Ovp factor has the highest significance for influence on the average stress response and the lowest for the average strain and impact strength. Interestingly its interaction with the contact geometry shows a more significant influence over the last two than the Ovp (see the P-Values in Table 2). The overlap degree between the female and male bodies increases the areas of horizontal contact by alternating the two materials at

the level of the boundaries. Even if the considered materials are dissimilar, the resulted zigzagging increases the maximum load capacity.

Ribeiro et al. studied the mechanical performance of multi-material 3D printed samples made of PLA and TPU with three macroscopic interfaces, U-shape, Dovetail, and T-shape, the latest showing the best results [5]. Similar results were obtained in this study, proving that macroscopic interfaces are a feasible solution for multi-material printing with dissimilar polymers. FFF allows the manufacturing of multi-material components in a single run. However, the materials combinations are limited to their chemical compatibility.

4 Conclusions

By defining a macroscopic interface between parts' mating bodies, the limitations of materials' compatibility are reduced. The influence of macroscopic contact interfaces was studied with three interlocking solutions. An overlap degree with three levels was also considered between the mating bodies.

Tensile and impact test results show that the mechanical properties are significantly improved regardless of the shape compared to the benchmark samples. The contact geometry and the interlocking side have the most significant influence from the considered parameters.

Macroscopic interfaces can introduce new possibilities regarding multi-material part manufacturing. However, further research should be done to explore new interface shapes and simplify their design process and implementation on complex parts.

References

1. Krishnanand, S.S., Nayak, A., Taufik, M.: Generation of tool path in fused filament fabrication. In: Agrawal, R., Jain, J.K., Yadav, V.S., Manupati, V.K., Varela, L. (eds.) Recent Advances in Smart Manufacturing and Materials. Lect. Notes in Mech. Eng. Springer, Singapore (2021).
2. Dey A, Roan Eagle I.N., Yodo, N., A review on filament materials for fused filament fabrication. J. Manuf. Mate. Process., 5(3), 69 (2021).
3. Lopes, L.R., Silva, A.F., Carneiro, O.S., Multi-material 3D printing: The relevance of materials affinity on the boundary interface performance. Addit. Manuf. 23, 45-52 (2018).
4. Ermolai, V., Sover, A., Nagîţ, G.: Influence of contact geometry over the filament bond of polylactic acid blends. In: Conf. Ser.: Mater. Sci. Eng., vol. 1235, 012004, (2021).
5. Ribeiro, M., Sousa Carneiro, O. and Ferreira da Silva, A., Interface geometries in 3D multi-material prints by fused filament fabrication. Rapid Prototyp. J. 25(1), 38-46 (2019).
6. Kluczyński, J., Śnieżek L., Kravcov, A., Grzelak, K., Svoboda, P., Szachogłuchowicz, I., Franek O., Morozov, N., Torzewski, J. Kubeček, P., The examination of restrained joints created in the process of multi-material FFF additive manufacturing technology. Materials, 13, 903 (2020).